



Title	Characteristics and mechanism on the distortion of friction stir welded aluminum alloy sheet
Author(s)	Yan, Dong-yang; Wu, Ai-ping; Silvanus, Juergen et al.
Citation	Transactions of JWRI. 2010, 39(2), p. 56-58
Version Type	VoR
URL	https://doi.org/10.18910/8096
rights	
Note	

The University of Osaka Institutional Knowledge Archive : OUKA

<https://ir.library.osaka-u.ac.jp/>

The University of Osaka

Characteristics and mechanism on the distortion of friction stir welded aluminum alloy sheet[†]

YAN Dong-yang ^{*}, WU Ai-ping ^{*}, SILVANUS Juergen ^{**}, ZHANG Zeng-lei ^{*} and SHI Qing-yu ^{*}

KEY WORDS: (Friction stir welding) (Residual distortion) (Numerical simulation) (Mechanical loads)

1. Introduction

As an advanced welding technology, possessing the characteristics of low heat input and solid-state joining, friction stir welding (FSW) has been widely used for joining aluminum alloys [1-2]. Although the residual stresses and distortion are smaller to those of traditional fusion welding, they still can not be ignored, especially when welding thin sheets with large size. Residual stresses in FSW have been widely investigated in recent years, and many conclusions have been obtained [3-9]. But few studies about distortion have been published.

Recently, a few papers [10-12] reported that when aluminum alloy sheets with large size were welded by FSW, it not only had remarkable out-of-plane distortion, but also had different distortion patterns from that of the arc welding with the same fixture conditions [12-13].

Many mechanical analysis models [6-9] have been developed to predict the residual stresses of FSW, but the stir tool's mechanical loads were not considered. The objective of this study is to investigate the characteristics and the reason for unusual distortion patterns of friction stir welded aluminum sheets, mainly by numerical simulation based on previous experimental studies.

2. Experimental procedures

FSW experiments were carried out to observe the distortions with butt welding 6056 aluminum alloy sheets of the 600×315×3 mm dimension. The dimensions of the stir tool were 13 mm in diameter of the shoulder, 5 mm in diameter of the pin, and 2.6 mm in length of the pin. The welding parameters were set to 1850 rpm in rotating speed and 700 mm/min in welding speed. Down load force of the stir tool was set to 8 kN, and forward tilt angle of the stir tool was kept at 2° during welding. The welding fixtures were made up of one backing board and two pressing boards. The temperature was measured by thermocouples which were embedded near the stir tool. Force and working torque of the stir tool were also recorded during the welding process. The measurements showed that the mechanical loads of stir tool mainly appeared as down force and working torque, which reached 8086 N and 8.76 Nm in

average respectively, while the loads in other two directions were very low. As shown in Fig. 1a, the main distortion of sheets after FSW was out-of-plane distortion, which was similar to an anti-saddle pattern. A three-coordinates measuring machine was used to measure the accurate distortion of the friction stir welded sheets [11]. The results showed that the offset between the highest and the lowest position of sheet was about 8.5 mm.

Fusion butt welding experiments were also executed on the aluminum alloy sheets with the same dimension and fixture conditions. The tungsten inert-gas (TIG) welding was utilized with the parameters of 16 V for voltage, 140 A for current and 4.42 mm/s for welding speed. The distortion shape of the sheets after TIG welding appeared as a saddle pattern (Fig.1b), which was opposite to the results of FSW.



Fig.1 Distortion pattern after welding, a) FSW, b)TIG

3. Finite element model

In order to compare the effects of the stir tool mechanical loads on the distortion, two analysis models are established. Model 1 considered the tool mechanical loads, while model 2 did not. Except for the difference on tool's mechanical loads, there were no other dissimilar conditions between the two models. ABAQUS/Standard software and sequentially coupled simulations were used. The geometry model and the meshing are shown in Fig. 2. All properties of Al 6056 used in simulation are temperature-dependent, even the yield strength is both temperature and temperature history dependent [14-16]. The dimensions of welding sheets and the FSW parameters were similar with experiments.

The total heat input was calculated with the equation of $Q = \eta M_z \omega$, where M_z was the working torque of the stir tool, and 8.76Nm was used, ω was the tangential speed of stir tool, η was the total heat coefficient, which was supposed to be 95% in simulation. It was assumed that heat

[†] Received on 30 September 2010

^{*} Tsinghua University, Beijing, China

^{**} EADS, Innovation Works Germany

Transactions of JWRI is published by Joining and Welding Research Institute, Osaka University, Ibaraki, Osaka 567-0047, Japan

input from the shoulder was 75% of the total, while the other was generated by the pin. The heat supplied by the tool shoulder was considered as a surface heat flux which is axi-symmetric and increases linearly with radius, and the heat generated by the pin was assumed to be a uniform volume heat flux [6, 8-9, 17-18].

The heat transfer condition on the sheet surfaces which were not in contact with the fixtures was set as the convection boundary condition, while on the contacting surfaces the heat transfer was treated in a way of contact heat conduction. The contact conductivity was assumed to be simply temperature-dependent [19].

The restriction effect of the welding fixtures on the sheet was set as a contact model, where the condition on contacting surfaces was described as Coulomb friction with a coefficient of 0.3, and the interaction force in the normal direction was set under the principle of "pressure-overclosure" [20]. The down force of the stir tool was imposed as a uniform surface pressure onto the upper surface of the sheet where the stir tool covered. The working torque was simplified as shearing friction between the shoulder surfaces and welded materials, and was treated as circumferential body forces, and applied on the uppermost layer integration points of the panels which lay in the region covered by tool shoulder [21]. Model 2 only has thermal load during mechanical analysis.

At the end of mechanical simulation, the restrictions of welding fixtures were removed. Thus the residual distortion of sheet appeared under unclamped condition.

4. Results and discussion

The computed and measured welding temperature histories of nodes A(X=300, Y=4.5, Z=3) and B(X=300, Y=14.5, Z=3) are displayed in **Fig. 3**. The computed results showed that the peak temperature in FSW was only 485°C, which was lower than the melting point of 6056 aluminum alloy.

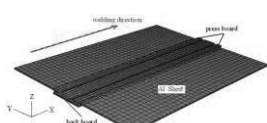


Fig.2 Geometric model and mesh for the welded sheets

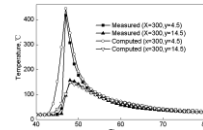


Fig.3 Computed and measured temperature results

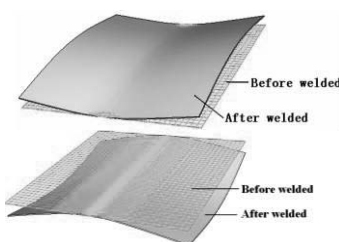


Fig.4 Distortion pattern with model 1(a) and model 2(b)

The distortion simulation results with the two analysis models are shown in **Fig. 4**. The patterns are different, anti-saddle shape for model 1, but saddle shape for model 2. These results indicated that the distortion obtained from the

model 1 was consistent with the FSW experimental results in shape, while the distortion shape from the model 2 was absolutely opposite. The offset between the highest and the lowest position of sheet was 7.41mm and 8.63mm in the model 1 and the model 2 respectively. These results indicated that the introduction of stir tool's mechanical loads had the effect of distortion reduction. The distortion curves on the line of X=40 mm, X=320 mm, X=560 mm, Y=-310 mm, Y=-116 mm and Y=0 mm on the top surface of the sheet from the computation with the model 1 and experimental results were listed in **Fig. 5**. The results showed that the distortion trends of the sheet by simulation and experimental results were consistent, and this consistency was compatible over the whole plate, not for some local positions. The largest error between the deformation values was less than 20%, which was acceptable in welding mechanical analysis. The distortion comparison confirmed that the model 1 was a reasonable model for distortion analysis of FSW.

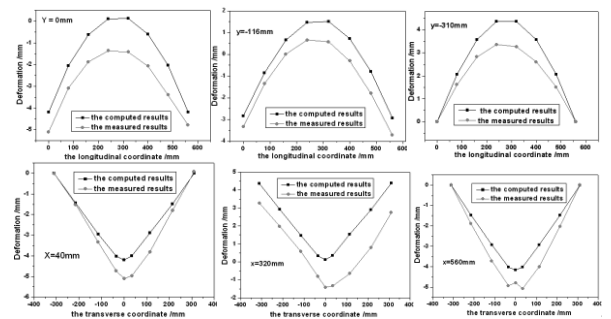


Fig.5 Deformation comparisons between simulation and experimental results

According to the residual transverse plastic strain results (**Fig. 6**) with the two models, mechanical loads of the stir tool not only reduced the residual plastic strain of the weld zone, but also changed the relationship of the magnitude of transverse plastic strain between top and bottom of the sheet. When the mechanical loads of the tool were not considered, like in model 2, the transverse compression plastic strain on sheet's top surface was smaller than that of the bottom surface, so the sheet became convex in width. But if the model included both thermal load and stir tool's mechanical loads, as in model 1, the transverse compressive plastic strain on sheet's top surface was larger than that of the bottom surface. Therefore, the distortion appeared concave shape in width of sheet.

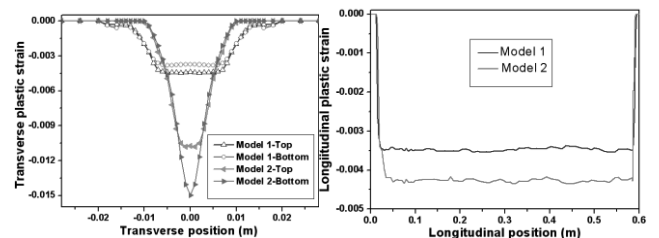


Fig.6 Distribution of transverse residual plastic strain

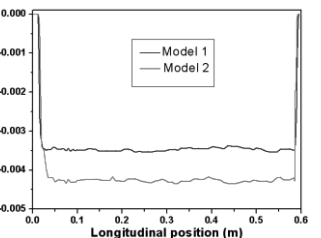


Fig.7 Distribution of longitudinal residual plastic strain

Curves in **Fig. 7** displayed the results of longitudinal plastic strain of the weld central line on the top surface with the two models, which appeared as compression strain. The strain curves comparison in the figure showed that the values of longitudinal compression strain were reduced under the impact of the stir tool's mechanical loads. This result could be approved by the value of longitudinal shrinkage of the weld seam by simulation: the shrinkage arrived at 0.8 mm with model 2, but this value fell to 0.3mm with model 1.

As is known, the materials in the welding zone can't expand and shrink freely during traditional fusion welding process under the local thermal load effect, so that some compressive plastic strain still remain after welding. In FSW process, the plastic strain is not only caused by thermal load, but also influenced by stir tool's loads. There are two main functions that these loads of the stir tool affect on the residual plastic strain. First, the tool's mechanical loads enhance the mechanical restriction effect on the materials around the stir tool, resulting in the lower residual plastic strain. Second, the down force of the stir tool supplies an additional compression, so the dimension of thickness direction in the stir zone was reduced. According to the volume constancy principle, the compression in thickness direction would bring additional expansion in the other two directions.

4. Conclusions

- (1) A 3D FEA model considering the stir tool's mechanical loads was developed to study the generation and characteristics of the distortion of friction stir welded aluminum alloy sheets.
- (2) The simulation results indicated that the functions of stir tool's mechanical loads could change the relationship of magnitude of transverse plastic strain between top and bottom surface of sheet, which was the key point to the difference of distortion patterns between FSW and fusion welding with the same fixture conditions.
- (3) Mechanical loads of the stir tool have two main functions to influence the distribution of residual plastic strain in FSW process, increasing the frictional resistance between the welded sheets and backing board, limiting the expansion of material in stir zone in thickness direction and bringing additional expansion in the plane of sheet.

Reference

- [1] W.M. Thomas, E.D. Nicholas, J.C. Need ham, M.G. Murch, P. Templesmith, C.J. Dawes, Friction Stir Welding, International Patent Application No. PCT/GB92102203 and Great Britain Patent Application No. 9125978.8, 1991.
- [2] R.S. Mishra, Z.Y. Ma: Mater. Sci. Eng., R 50, 2005, 1-78
- [3] M. James, M. Mahoney: Proc. of 1st Int. Symposium on Friction Stir Welding, Thousand Oaks, CA, USA, June 14-16, 1999.
- [4] C.D. Donne, E. Lima, J. Wegener, A. Pyzalla, T. Buslaps: Proc. of 3rd Int. Symposium on Friction Stir Welding, Kobe, Japan, September 27-28, 2001.
- [5] S.R. Rajesh, Han Sur Bang, Woong Seong Chang, Woong Seong Chang, HeungJu Kim, et al. J. Mater. Process. Technol., 2007(187 & C188): 224-226
- [6] M. Z. H. Khandkar, A. K. Jamil, P. R. Anthony, A. S. Michael, et al. J. Mater. Process. Technol., 2006, 174(1-3):195-203
- [7] Ting Li, Qing-yu Shi, Hong-ke Li: Sci. Technol. Weld. Join., 2007,12(8), 664-670
- [8] Qing-yu Shi, Terry Dickerson, Hugh R. Shercliff: Proc. 6th Int. Conf. on Trends in Welding Research, Pine Mountain, Georgia, USA, April 2002.
- [9] T.L.Dickerson, Q.Y. Shi, H.R.Shercliff: Proc. 4th Int. Symp. On Friction Stir Welding, Salt Lake City, Utah, USA, May 2003.
- [10] D. A. Price, S. W. Williams, A. Wescott, C. J. C. Harrison, A. Rezai, A. Steuwer, M. Peel, P. Staron4 and M. Kocak. Sci. Technol. Weld. Join., 2007, 12 (7): 620-633.
- [11] Q.Y. Shi, J. Silvanus, Y. Liu, et al. Sci. Technol. Weld. Join., 2008, 13 (5): 472-478.
- [12] S.R.Bhude, P. Michaleris, M. Posada, J. Deloach. Welding Journal, 2006, 85(9):189-195.
- [13] C.L.Tsai, S.C.Park, W.T.Cheng. Welding Journal, 1999, 78(5):156-165.
- [14] G. Grimvall, Thermophysical properties of materials, New York, 1999.
- [15] J. E. Parrott, D. S. Audrey, Thermal Conductivity of solids, Pion, London, 1975.
- [16] Z. L. Zhang, J. Silvanus, H.K. Li, Q.Y. Shi, Sci. Technol. Weld. Join., 2008, 13 (5): 415-421.
- [17] M. Z. H. Khandkar, J. A. Khan, A. P. Reynolds: Sci. Technol. Weld. Join., 2003(8): 165-174.
- [18] T. Vuyst, L.D. Dealvise: Proc.5th Int. Symp. on Friction Stir Welding, France, 2004.
- [19] Chuan-song Wu: Numerical analysis for heat transfer in welding process, Harbin institute of technology press, Harbin, China, 1990.
- [20] ABAQUS/Standard User's Manual, ver. 6.5.
- [21] Ting Li, Qing-yu Shi, Hong-ke Li, Wei Wang, Zhi-peng Cai: International Welding Joining Conference-Korea 2007, COEX Convention Center, Seoul, Korea, May 10-12, 2007.